Vol. **112** (2007) *ACTA PHYSICA POLONICA A* No. 2

Proceedings of the XXXVI International School of Semiconducting Compounds, Jaszowiec 2007

Preparation and Optical Properties of $Zn_{1-x}Mn_xTe_{1-y}O_y$ Highly Mismatched Alloy

A. Avdonin[a], Le Van Khoi[a], W. Pacuski[b], V. Domukhovski[a] and R.R. Gałązka[a]

[a]Institute of Physics, Polish Academy of Sciences
al. Lotników 32/46, 02-668 Warsaw, Poland
[b]Institute of Experimental Physics, Warsaw University
Hoża 69, 00-681 Warsaw, Poland

The $Zn_{1-x}Mn_xTe_{1-y}O_y$ alloy was prepared using a rapid crystallization technique. X-ray diffraction measurements were used to estimate the oxygen doping level. It is demonstrated that the oxygen solubility in $Zn_{1-x}Mn_xTe_{1-y}O_y$ alloys greatly depends on the manganese concentration. No oxygen related effects were observed in the manganese free samples. The highest value of the oxygen molar fraction (y) achieved in the present study was 0.0023 in a sample having manganese fraction (x) of 0.056. The decrease in the alloy band gap was observed with increasing oxygen content. The oxygen-related trap level in $Zn_{1-x}Mn_xTe_{1-y}O_y$ was found to be strongly shifted with respect to that in $ZnTe_{1-y}O_y$. The shift is assigned to the creation of complex (Mn_xO) traps.

PACS numbers: 61.66.Dk, 61.72.Vv, 78.55.–m

1. Introduction

The $Zn_{1-x}Mn_xTe_{1-y}O_y$ (ZMTO) alloy has attracted attention recently due to its possible photovoltaic applications [1]. It is stated that incorporation of a small fraction (< 2 at.%) of oxygen atoms into the $Zn_{1-x}Mn_xTe$ (ZMT) lattice produces a large conduction band splitting and results in the formation of a narrow band of extended states within the band gap of ZMT alloy. Thus there are two conduction bands in the ZMTO band structure and thereby there are two direct band gaps. The existence of such material is very promising for multi-band single-junction solar cells applications.

The $Zn_{1-x}Mn_xTe_{1-y}O_y$ alloy belongs to the group of highly mismatched alloys [1]. In such alloys the anions are partially replaced by highly electronegative isoelectronic atoms. The most famous examples of highly mismatched alloys are III–N–V and II–O–VI ternary alloys, such as GaNAs or ZnOTe, where the anions are being replaced by nitrogen and oxygen atoms, respectively. The interest in the highly mismatched alloys stems from their unusual compositional band gap behavior. The examples of such behavior are the band bowing effect and the band anticrossing effect [2]. It is predicted that between II–O–VI alloys the $ZnTe_{1-y}O_y$ (ZTO) alloy should have the most pronounced effect because among group-VI elements the O and Te have the highest difference of the electronegativity [3] (3.44 and 2.1, respectively).

In the present paper an attempt was made to synthesize the ZMTO alloys using a rapid crystallization technique. The Mn was needed to facilitate the oxygen incorporation in ZnTe. The advantage of such approach is that it permits to estimate the solubility of the oxygen in ZMT and provides bulk samples. In the previous publications only thin layers could be made.

2. Experimental details

The synthesis was carried out in the closed vacuumed silica ampules using ZnTe, MnTe, and ZnO compounds as source materials. The ampules were heated up to 1450°C and were held at that temperature for five hours to achieve a better homogenization of the material. After that the ampules were rapidly cooled down by removing from the hot region of the furnace. The whole process was carried out in the nitrogen gas atmosphere under the pressure of 5 bar. The external pressure was needed to compensate the pressure of the material vapor inside the ampules and to maintain the shape of the softened quartz glass. Since the ampules were not coated with the graphite, the Mn reaction with the silica walls could not be avoided.

Usually when using Mn-compound as the precursor the ampule is being coated from the inside with a thin layer of graphite to avoid the Mn reaction with the silica walls. However, in the present work such measure could not be applied because in the presence of ZnO it resulted in the formation of CO_2 gas of a high pressure and prevented oxygen incorporation. Thus the graphite coating could not be used.

The rapid crystallization method was used in order to avoid impurity segregation along the ingot and to limit the oxygen diffusion.

The resulting material has the form of polycrystalline ingots 10–14 mm in diameter and about 60 mm long. The grain size was about 0.1–1 mm. For the optical measurements the samples were cut into 1 mm thick slices and polished mechanically and chemically in Br–methanol solution. No additional treatment was applied.

X-ray powder diffraction (XRD) was used to study the quality of the samples and the amount of the incorporated oxygen. The measurements were performed on

a Siemens "D5000" diffractometer with Cu K_α ($\lambda = 1.54184$ Å) radiation. The Mn concentration in the samples was measured using energy-dispersive X-ray (EDX) analysis. The oxygen concentration could not be measured by EDX because our EDX apparatus was not sensitive to elements lighter than Si.

In addition to structural studies the reflectivity (R) and photoluminescence (PL) measurements have been performed.

Two sets of samples having different initial fractions of Mn and O have been prepared. In the first set the Mn concentration was held constant (5%) and the O concentration was varied (0–15%). In the second set of samples the O concentration was held constant (5%) and the Mn concentration was varied (0–7%).

The first thing, which ought to be noticed here, is the decreasing concentration of incorporated Mn with increasing initial oxygen content (sample set no. 1) despite the fact that MnTe has a very high solubility in ZnTe ($0 < x < 0.86$) [4, 5]. The Mn is being extracted from the solution into a reddish compound covering the walls of the ampule. The amount of the extracted Mn depends on the ZnO fraction and is not caused only by the Mn reaction with silica walls.

3. X-ray diffraction

The powder X-ray diffraction diagrams confirm that the material has the zinc-blende structure and no additional phases are present. The analysis of the experimental data is complicated by the fact that both manganese and oxygen concentrations are being varied. To estimate the amount of incorporated oxygen one should compare the lattice constants of the doped and oxygen-free samples. The

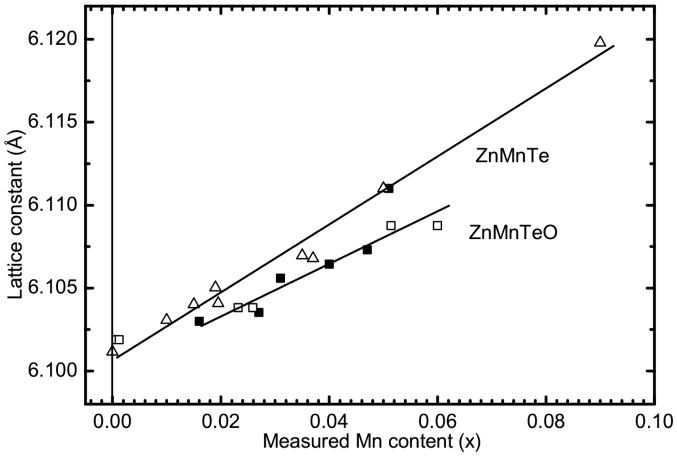

Fig. 1. The dependence of the lattice constant on the manganese concentration. Open triangles: oxygen free samples $Zn_{1-x}Mn_xTe$ used as the reference. Filled squares: data for samples from set no. 1. Open squares: data for samples from set no. 2. The left-most data point: manganese free sample.

dependence of the lattice constant on the manganese concentration is presented in Fig. 1 for both doped (squares) and oxygen-free samples (triangles). Three facts should be noticed here.

First, the oxygen containing samples have a smaller lattice constant. This confirms oxygen incorporation into the lattice. According to Vegard's rule the shift of the lattice constant value should be directly proportional to oxygen concentration.

Second, the oxygen concentration (as well as the shift of the lattice constant) increases with increasing manganese concentration.

Third, there is no shift in the manganese free sample doped with oxygen (the left-most data point in the figure). This confirms that the presence of manganese is essential for successful oxygen doping and the oxygen concentration is proportional to the manganese concentration.

Assuming that the Vegard rule for lattice constants is valid in our case, the value of the oxygen concentration can be estimated from the relation

$$a^{\mathrm{ZMTO}} = a^{\mathrm{ZMT}}(1-y) + a^{\mathrm{ZMO}}y. \tag{1}$$

It was found that the oxygen concentration increases linearly with increasing manganese content and the highest oxygen fraction achieved so far was 0.0023 (4×10^{19} cm^{-3}).

4. Optical properties

4.1. Reflectivity

The free exciton reflectance spectra were measured in order to observe the band bowing effect. Despite the fact that the reflectivity was measured on the polished polycrystals the excitonic feature of the spectrum is clearly visible. As an example the free exciton reflectivity spectra are presented in Fig. 2 (inset) for two samples, the ZMTO sample and oxygen-free ZMT sample. Since the two presented samples have almost the same manganese molar fraction (0.056 and 0.051, respectively) one can state that the shift of the free exciton position (about 16 meV) is caused by the substitutional oxygen. The observed shift may be explained by both band bowing effect and the variation of the free exciton binding energy. Since the oxygen molar fraction is small and the data on free exciton bonding energy in ZMTO is not available and since the band bowing effect in ZMTO is predicted to be very strong [3], the dependence of the exciton bonding energy on the oxygen molar fraction was neglected in the further discussion.

Since the free exciton energy depends on both manganese and oxygen concentrations it is necessary to separate the effect of the substitutional oxygen. The data on the dependence of the free exciton energy on the manganese concentration in ZMT is available [6, 7] and can be expressed using the relation

$$E_x^{\mathrm{ZMT}} = E_x^{\mathrm{ZnTe}} + \Delta E_x x, \tag{2}$$

where $\Delta E_x = 0.68$ eV, E_x denotes the free exciton energy and x denotes the Mn molar fraction. Since the oxygen molar fraction is small the same relation should

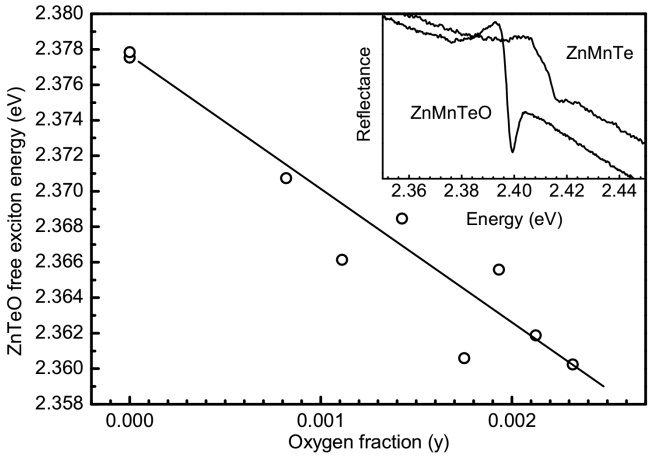

Fig. 2. Calculated dependence of the ZTO free exciton energy vs. oxygen molar fraction. Inset: The comparison of the free exciton reflectivity spectra for two samples, with and without oxygen, having the same Mn concentration ($x = 0.05$).

be applicable in the case of ZMTO

$$E_x^{\mathrm{ZMTO}} = E_x^{\mathrm{ZTO}} + \Delta E_x x. \tag{3}$$

Hence one can calculate the ZTO free exciton energy. The results are presented in Fig. 2. It is seen that the ZTO band gap decreases with increasing oxygen content. Thus the bowing effect once again confirms the presence of the oxygen in the samples.

4.2. Photoluminescence

The PL spectrum of the ZMTO alloy is presented in Fig. 3a. It is dominated by a wide intensive band centered at 1.65 eV (750 nm). This band is the characteristic feature of the ZnMnTeO alloy since it was not ever observed neither in ZnMnTe nor in ZnTeO alloys. The manganese-related band in ZnMnTe is located at 1.95 eV (630 nm) and it is being attributed to manganese inner *d*-shell electron transitions. The oxygen-related band in ZnTe:O is located at 1.88 eV (660 nm) (Fig. 3b) and is caused by the annihilation of the oxygen-bound exciton [8]. Though the band has the excitonic nature it is a very wide band, formed of numerous phonon replicas of the non-phonon line. At relatively high oxygen concentrations the non-phonon line is not visible at all [9] and only overlapping phonon replicas are present. This overall band is shifted with respect to the non-phonon line by $\Delta E = 0.09$ eV.

Though the discussed band is shifted by about 230 meV with respect to both these bands (manganese and oxygen-related), the facts suggest that the band has also the oxygen-bound exciton nature. The shift of the band is caused by the presence of manganese and the appearance of some new complex states. Such

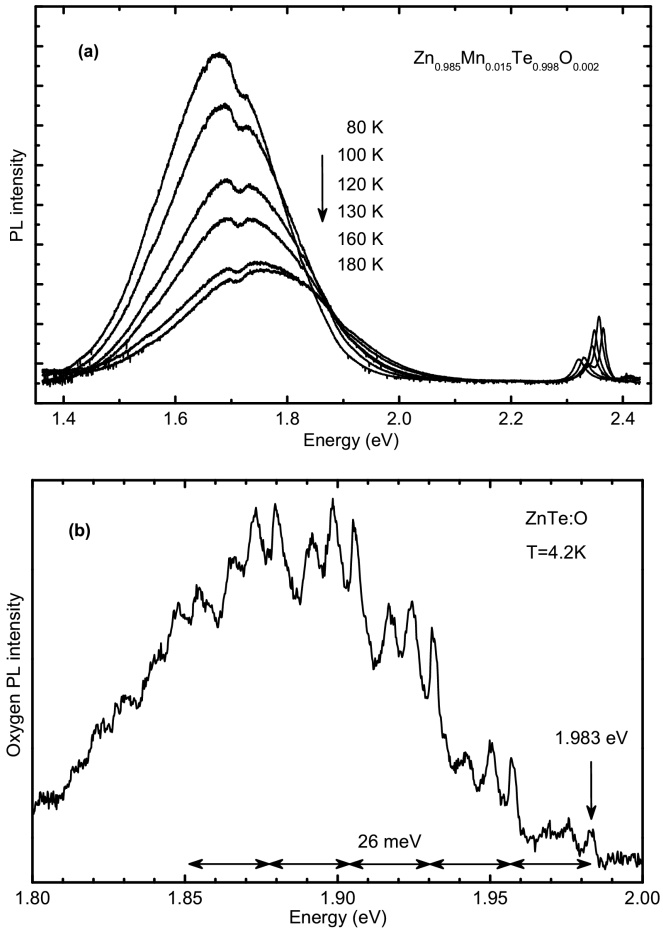

Fig. 3. (a) The PL spectra of the ZMTO sample at different temperatures. (b) The PL spectra of the ZnTe:O sample. The oxygen-bound exciton is located at 1.983 eV and the broad band is formed of its phonon replicas.

centers are believed to contain one oxygen atom and one (or more) manganese atoms and will be further denoted as (Mn_xO).

The oxygen-bound exciton in ZnTeO is formed of an electron tightly trapped on the deep oxygen trap and a hole bound weakly to the negatively charged oxygen trap by the Coulomb field [10, 8]. It is demonstrated [10] that the hole binding energy of such exciton is about 5.7 meV and the electron binding energy is about 0.4 eV. Thus the alteration of the structure of the electron trap (e.g. by adding one manganese atom) should change the electron activation energy but should not affect much the hole binding energy since the charge of the trap will remain unchanged. This model is confirmed by the PL temperature quenching experiment. It was found that indeed in the range of 60–100 K the activation energy of the PL temperature quenching is about 5 meV.

The complex shape of the band (Fig. 3a) suggests that the band consists of a number of narrower bands. Hence one can presume that there are a number of electron traps with different depths. The centers responsible for those traps should be formed of one oxygen atom and a number of manganese atoms. Indeed, it was mentioned earlier that the oxygen concentration is directly proportional to the manganese concentration. Hence the oxygen atom should always be located in the vicinity with the manganese atom. Since the oxygen concentration is much smaller than the manganese concentration, the probability to have two close oxygen atoms is small.

Another feature worth being mentioned is the unusual blue-shift of the overall band maximum with temperature (Fig. 3a). With increasing temperature the low-energy slope of band quenches faster than the high-energy slope. The blue--shift of the band then might be explained by the difference of the hole binding energy between different traps. If deeper traps have a smaller hole binding energy, then the excitons bound to those traps will be ionized first. Since those excitons have a smaller energy of the emitted photon, the maximum of the wide combined band will shift toward higher energies.

The deconvolution of the considered band into the components provided at least two bands centered at 1.88 and 1.73 eV. The energy depth of the respective electron traps may be calculated from the formula: $E = E_{\mathrm{g}} - E_{\mathrm{PL}} - \Delta E$. Thus the position of the electron traps was found to be about 0.58 and 0.76 eV below the conduction band minimum, respectively. This levels are attributed to discussed complex ($\mathrm{Mn}_x\mathrm{O}$) centers.

The hypothesis that the manganese atoms should change the energy position of the oxygen trap in ZnMnTeO is supported by the recent report on *ab initio* calculation of the oxygen trap [11] in II–VI compounds. The authors demonstrated that the energy level of the oxygen trap is strongly influenced by the nearest neighbor cation atoms.

Thus the oxygen-related trap level in ZnMnTeO is situated lower than the corresponding trap in ZnTeO. The importance of this result is due to the fact that the application of the band anticrossing model to the ZnMnTeO alloy strongly depends on the energetic position of the oxygen trap. Hence the interpretation of the experimental results (e.g. in [1, 5]) may be changed since the authors assumed that in ZMTO the oxygen trap has the same depth as in ZTO.

5. Conclusions

The results confirmed the fact that the manganese greatly increases the oxygen solubility in ZnTe. The doping level as high as 4×10^{19} cm^{-3} (0.0023 oxygen molar fraction) was obtained using doping from the melt phase. The reported value is one hundred times greater than the oxygen solubility in pure ZnTe [10]. No oxygen incorporation was observed without additional manganese doping. The reduction of the manganese molar fraction was observed with increasing initial oxygen concentration in the ampule charge.

The band bowing effect, which confirms the oxygen incorporation, was observed in the free exciton reflectivity measurements. A model is proposed to describe the strong shift of the oxygen-bound exciton band in the photoluminescence spectrum. According to the model new complex oxygen-related traps (Mn_xO) appear in the band gap of the $Zn_{1-x}Mn_xTe_{1-y}O_y$ alloy in the presence of Mn atoms. The (Mn_xO) traps are located at 0.58 and 0.76 eV below the conduction band minimum.

References

[1] K.M. Yu, W. Walukiewicz, J. Wu, W. Shan, J.W. Beeman, M.A. Scarpulla, O.D. Dubon, P. Becla, *Phys. Rev. Lett.* **91**, 246403 (2003).

[2] W. Shan, W. Walukiewicz, J.W. Ager III, E.E. Haller, J.F. Geisz, D.J. Friedman, J.M. Olson, S.R. Kurtz, *Phys. Rev. Lett.* **82**, 1221 (1999).

[3] Chang-Youn Moon, Su-Huai Wei, Y.Z. Zhu, G.D. Chen, *Phys. Rev. B* **74**, 233202 (2006).

[4] A. Pajaczkowska, *Prog. Cryst. Growth Charact.* **1**, 289 (1978).

[5] J.K. Furdyna, *J. Appl. Phys.* **64**, R29 (1988).

[6] A. Twardowski, P. Swiderski, M. von Ortenberg, R. Pauthenet, *Solid State Commun.* **50**, 509 (1984).

[7] A. Twardowski, *Phys. Lett.* **94A**, 103 (1983).

[8] J. Hopfield, D.G. Thomas, R.T. Lybch, *Phys. Rev. Lett.* **17**, 312 (1966).

[9] Z.T. Kang, H. Menkara, B.K. Wagner, C.J. Summers, R. Dust, Y. Diawara, G. Mednikova, T. Thorson, *J. Electron. Mater.* **35**, 1262 (2006).

[10] J.D. Cuthbert, D.G. Thomas, *Phys. Rev.* **154**, 763 (1967).

[11] Jingbo Li, Su-Huai Wei, *Phys. Rev. B* **73**, 041201 (2006).